



1 **Aircraft-based observation of volatile organic compounds**
2 **(VOCs) over the North China Plain**

3 Yibo Huangfu^{1,#}, Ziyang Liu^{1,#}, Bin Yuan^{1,*}, Sihang Wang¹, Xianjun He¹, Wei Zhou²,
4 Fei Wang², Ping Tian², Wei Xiao², Yuanmou Du², Jiujiang Sheng^{2,*}, Min Shao¹

5 ¹ College of Environment and Climate, Institute for Environmental and Climate
6 Research, Guangdong-Hongkong-Macau Joint Laboratory of Collaborative Innovation
7 for Environmental Quality, Jinan University, Guangzhou 511443, China

8 ² Beijing Weather Modification Center, Beijing 100089, China

9 [#] These authors contributed equally to this work

10 ^{*} Corresponding author: Bin Yuan (byuan@jnu.edu.cn), Jiujiang Sheng
11 (jiujiangsheng@163.com)



12 **Abstracts.**

13 The vertical distribution of reactive trace gases can greatly help understand the complex
14 atmospheric evolution under the joint impacts of surface emission, chemical removal,
15 and regional transport. Focusing on the core area of the North China Plain, aircraft-
16 based observations were conducted to reveal the vertical distributions of volatile
17 organic compounds (VOCs) measured by high-time resolution mass spectrometry.
18 Generally decreasing trends of VOC concentrations with altitudes were captured,
19 indicating strong surface source emissions and chemical removal within the planetary
20 boundary layer (PBL). Ethanol exhibited the highest concentration within the PBL with
21 an average of 46.7 ppbv and the largest ratio (16.5) between the average below and
22 above the PBL heights. The vertical-averaged VOCs above Baoding were greater than
23 those in Beijing by factors ranging from 1.2 to 3.5, suggesting richer precursors for
24 secondary pollutant formation in Baoding. Increases of several VOC species, including
25 styrene and acetonitrile, at high altitudes (>2500 m) were captured in Beijing.
26 Correlation analysis further revealed the significant influences of industrial and
27 biomass burning emissions. Our results highlight the critical role of both local
28 emissions and regional transport in shaping the VOC vertical distributions, which may
29 affect atmospheric organic chemistry across various atmospheric layers in the region.

30 **Keywords:** Vertical profiles; aircraft-based observation; volatile organic compounds

31



32 **1 Introduction**

33 The North China Plain (NCP) stands as one of the most developed city clusters
34 in China, yet it is also a region of concern that suffers from severe air pollution (Zhao
35 et al., 2021; Yao et al., 2022; Le et al., 2020; Wang et al., 2023). Following the
36 implementation of the Action Plan on the Prevention and Control of Air Pollution, the
37 particulate matter concentrations in NCP have significantly declined, primarily due to
38 a sharp reduction in anthropogenic emissions, however, ozone levels have not shown a
39 similar downward trend (Chen et al., 2020; Li et al., 2019a; Lu et al., 2019; Lu et al.,
40 2020). From 2013 to 2019, the annual maximum daily average of 8-h ozone (MDA8O_3)
41 concentrations increased significantly with a rate of 2.3 ppbv yr^{-1} in Beijing (Chen et
42 al., 2020), while during warm seasons (Apr. – Sep.), the average increasing rate reached
43 3.3 ppbv yr^{-1} for NCP (Lu et al., 2020). Under the background of coordinated efforts to
44 reduce pollution and carbon emissions, the continuous improvement of ambient air
45 quality in the NCP region is under great pressure.

46 Volatile organic compounds (VOCs), as the key precursors of ozone and
47 secondary organic aerosols due to photochemical degradation, have been listed as one
48 of the key indicators for atmospheric environmental quality during the "14th Five-Year
49 Plan" period (Li et al., 2022b; Mao et al., 2021). The temporal variation, emission
50 characteristics, and environmental effect of VOCs have been extensively studied in the
51 NCP region through ground-based measurements, greatly enhancing the understanding
52 of the role in the formation of photochemical pollution (Yuan et al., 2012; Wang et al.,
53 2014; Li et al., 2019b; Zhao et al., 2021; Sun et al., 2018; Forster et al., 2023). However,
54 recent studies have also revealed the complex evolution of VOCs in the atmosphere
55 under the impact of meteorological conditions (Zhang et al., 2018; Shi et al., 2018) and
56 inter-city and regional transport (Liu et al., 2019; Zhao et al., 2021; Chang et al., 2019)
57 that cannot be thoroughly investigated based on ground measurements.

58 In the past few years, vertical observations have been carried out utilizing
59 observation towers (Zhang et al., 2020; Li et al., 2022a; Yang et al., 2024; Li et al., 2024),
60 tethered balloons (Zhang et al., 2019; Sangiorgi et al., 2011; Zhang et al., 2018),
61 unmanned aerial vehicles (UAVs) (Peng et al., 2015; Han et al., 2016; Vo et al., 2018),
62 and aircraft (Benish et al., 2020; Forster et al., 2023; Zhao et al., 2021; Wilde et al., 2021),
63 bringing the opportunity to study VOCs from a three-dimensional perspective.
64 Compared to other vertical observation techniques, aircraft platforms offer distinct



advantages, including the capability of covering larger spatial areas, carrying heavy instrument payloads, and performing both vertical and horizontal observations at higher altitudes (Kwak et al., 2020;Zhao et al., 2021;Dieu Hien et al., 2019). The advantages of aircraft measurement make it an irreplaceable role in scientific research and practical applications. While aircraft-based research has been conducted intensively in the United States and Europe with high temporal resolution instruments (Fisher et al., 2016;Karion et al., 2015;Ren et al., 2018), only a handful of similar aircraft flights have been conducted equipped with online instruments that measure inorganic pollutants and aerosols in China (Zhao et al., 2021;Liu et al., 2018). Limited aircraft-based VOC measurements in China typically applied the collection of canister samples followed by detection by gas chromatography techniques in the laboratory (Xue et al., 2011;Benish et al., 2020;Liu et al., 2013). However, the vertical distribution of VOCs in the NCP region is still unclear due to the scarcity of offline samples, hindering the ability to accurately assess the impacts of local emissions and air mass transport on VOC levels.

This study analyses aircraft-based observation results over the Beijing and Baoding area, the two core cities of the NCP region. A proton transfer reaction time-of-flight mass spectrometer (PTR-ToF-MS) was equipped on the platform to monitor VOC concentrations with high time resolution across altitudes. Combined with correlation analysis of VOC pairs, possible sources and origins of VOCs within the planetary boundary layer (PBL) and the atmosphere above it were discussed, pointing out the important roles of local urban emissions and regional transport.

2 Methods

2.1 Aircraft flight routes

A King Air 350ER aircraft (Hawker Beechcraft) was deployed and five flights were conducted between Sep. 9th and 15th in 2017, and an additional flight on July 14th, 2019. The flight trajectories are summarized in **Table 1** and illustrated in **Figure 1**. The aircraft was based at Shahe Airport (40°8'24" N, 116°19'48" E) in Changping District, Beijing, surrounded by villages, factories, and educational institutions. Four of the flights in 2017 (Sep. 9th, 12th, 13th, and 15th) focused on the Beijing area, while the remaining two flights (Sep. 14th, 2017, and Jul. 14th, 2019) followed southwest trajectories over the forest area before turning southeast to the Baoding area and returning to Shahe Airport. During each flight, the aircraft maintained level flight at a given altitude before ascending or descending to the next predetermined flight level.



98 The step intervals between altitudes were consistently maintained within approximately
99 150 to 200 meters.

100 **2.2 VOC sample and meteorological data collection**

101 A PTR-ToF-MS (PTR-ToF-MS-8000, Ionicon Analytik GmbH, Austria) was
102 applied onboard to measure VOC concentrations during each flight. The time-of-flight
103 mass spectrometry has been proven to have the capability of measuring VOCs at high
104 time resolution over broad mass spectra (Wu et al., 2020a; Yuan et al., 2017). Ambient
105 air was introduced into the sampling device and then subsampled by the PTR-ToF-MS
106 using Polytetrafluoroethylene (PTFE) tubing. With a voyage speed of ~250 km/h of the
107 aircraft, VOC concentrations were measured every 5 s, resulting in a spatial resolution
108 of ~70 m. The PTR-ToF-MS was operated with a drift pressure of 2.2 mbar, E/N 135
109 Td, and reactor temperature of 60 °C. The raw spectral data of PTR-ToF-MS were
110 processed using the Ionicon Data Analyzer (IDA, V2.0.1.0), including mass calibration,
111 peak detection, peak fitting, and etc. The sensitivities of PTR-ToF-MS for various VOC
112 species were calibrated with commercial standard gas (Apel-Riemer, Environmental
113 Inc., USA). A total of 15 VOC species are reported in this study and listed in **Table S1**.
114 Based on the multi-level tests in the laboratory, the impacts of humidity on VOC
115 sensitivities were evaluated to be less than 10% for the reported VOC species, so no
116 correction was conducted. In addition, the aircraft platform also carried instruments that
117 recorded the meteorological parameters (AIMMS-20, Aventech Research Inc.),
118 including temperature, relative humidity, and pressure. A global positioning system
119 (GPS) was equipped to record the aircraft's position. All instruments were thoroughly
120 inspected and air-tightly checked before each flight to ensure the quality and reliability
121 of data. To minimize the impact of aircraft exhaust emissions on VOC measurement,
122 the data measured during the first 2 minutes after the engine started were excluded from
123 the profile data.

124 **2.3 Height of planetary boundary layer**

125 In this study, the height of planetary boundary layer (HPBL) was determined by
126 the air parcel method (Zhao et al., 2020; Zhao et al., 2019), which was considered to be
127 more accurate and less deviated by human subjective judgment compared with the
128 visual observation method and data simulation method (Zhang et al., 2019). The air
129 parcel method determines the HPBL based on the vertical profile change of the potential



130 temperature (T_θ) during the adiabatic process when the air mass reaches the reference
131 pressure (1000 hPa). The calculation formula of T_θ is:

$$132 \quad T_\theta = T \left(\frac{1000}{P} \right)^{\frac{R_d}{C_{pd}}}$$

133 where P is the air pressure, T is the temperature under different air pressures, and R_d/C_{pd}
134 is taken as 0.286 in this study (Zhang et al., 2018). The vertical profiles of
135 meteorological factors are shown in **Figure S1**. The HPBL during each ascending and
136 descending stage is listed in **Table S2**. A 10% uncertainty is determined based on
137 previous studies (Zhao et al., 2019; Zhang et al., 2014; Vogelezang and Holtslag, 1996).

138 **3 Results and discussion**

139 **3.1 The characteristics of VOC vertical distributions in Beijing**

140 The ambient air quality data of criteria pollutants (ozone, NO_2 , SO_2 , CO, $\text{PM}_{2.5}$,
141 and PM_{10}) of Changping Town station, the nearest national air quality monitoring
142 station to the Shahe Airport, were collected from the China National Environmental
143 Monitoring Center (CNEMC) and presented in **Figure 2**. According to the Level-II
144 NAQS thresholds, pollution events in Beijing with $\text{PM}_{2.5}$ exceedances on Sep. 9th, 10th,
145 and 14th and ozone exceedances on Sep. 13th were noticed. The vertical profiles of
146 relative humidity (RH), temperature (T), and T_θ in **Figure S1** provide meteorological
147 information for each flight. Monotonic trends for T and T_θ were recorded. T decreased
148 with altitude, while T_θ had opposite trends. In contrast, RH showed a more complex,
149 non-monotonic trend with altitude, with great variations found across different aerial
150 surveys, reflecting the complexity of the boundary layer structure.

151 Five flights were conducted over Beijing in Sep. 2017. The averaged
152 concentrations of all 15 VOC species ranged from 25.9 ± 13.4 ppb to 52.1 ± 57.7 ppb
153 (**Table S3**). As illustrated in **Figure 3**, the VOC concentrations within the PBL (**Table**
154 **S4**) were compared with previous measurements in urban Beijing (Squires et al.,
155 2020; Yuan et al., 2012). The concentrations of aromatic species below the PBL in this
156 study were comparable to those measured in 2010 (**Figure 3b**), with data points
157 clustering along the 1:1 line. For the OVOC species, the differences remained within
158 or close to twofold variations. By contrast, compared with the 2017 measurement, the
159 aromatic species measured in this study were higher by factors ranging from 3.2 to 6.2
160 (**Figure 3c**). Measurements in 2017 were made at the IAP meteorology tower
161 represented the VOC concentrations driven by traffic-related emissions in the center of
162 urban Beijing (Squires et al., 2020), while the VOC measured in aerial surveys in this



163 study might be under the impact of industrial emissions from the suburban region,
164 especially at lower altitudes. Most OVOC species measured across both campaigns
165 showed good agreement within twofold variability, except methyl ethyl ketone (MEK),
166 which exhibited a factor of 5.7 higher in this study. As one of the common ingredients
167 in industrial solvents, MEK can be emitted through multiple industrial processes (Wu
168 et al., 2020b; Wang et al., 2024) and higher concentrations in this study are likely
169 attributable to the nearby industrial emissions. Regarding the biogenic species, isoprene,
170 methyl vinyl ketone and methacrolein (MVK&MACR), and monoterpenes measured
171 in this study were consistently higher than those reported in the other two campaigns,
172 probably due to the enhanced biogenic emissions from the suburban region surrounded
173 by mountain vegetation (**Figure 1**).

174 The characteristics of VOC vertical distributions were investigated through ten
175 profiles obtained across the five flights over Beijing in 2017. Composite profiles of
176 individual VOC species, as shown in **Figure 4**, revealed fundamental vertical
177 distribution patterns, with detailed profiles for each flight provided in **Figures S2-S6**.
178 Generally, decreasing trends with altitudes were observed for most VOC species, and
179 the largest concentration variations were noticed towards the surface due to the dynamic
180 change of surface emissions.

181 All aromatic hydrocarbons exhibited characteristic negative vertical gradients
182 with maximum concentrations at ground level (0.3-4.5 ppbv by average) and
183 progressive decreases through the PBL, except the anomalous profile of styrene
184 (**Figure 4**). Aromatic hydrocarbons primarily originate from vehicular and industrial
185 emissions, and their lifetime within the PBL can span several days. The dominance of
186 surface emissions explains their significantly higher concentrations near the ground
187 than those measured above the the PBL. As turbulent mixing transports air upward,
188 these compounds get oxidized with OH radicals, diminishing to near-zero levels at
189 higher altitudes with minimal variation. The ground levels of C8 aromatics were the
190 highest, reaching 4.5 ppbv on average. In contrast to other aromatic hydrocarbons,
191 styrene displayed a distinct increase with altitude above the PBL, peaking notably at
192 ~3500 m. Similar concentration enhancements at the same altitude were also observed
193 for methanol, acetonitrile, and acetaldehyde. This anomalous profile, potentially
194 associated with upper-air biomass burning plumes or long-range transported industrial
195 emissions, will be further explored in **Section 3.3**.



OVOCs originate from both biogenic and anthropogenic sources and can also be formed as secondary products during the oxidation of non-methane hydrocarbons, complicating the interpretation of their vertical distributions (Yuan et al., 2012). Near the surface, OVOC concentrations were substantially higher than those of aromatic hydrocarbons. Across all flights, the vertical profiles of both alcohols and MEK followed trends similar to aromatic hydrocarbons. Their vertical variations demonstrate the impact of PBL dynamics, as evidenced by their pronounced vertical gradients (**Figure 4**). During the flight on Sep. 12th, the HPBL over Beijing exhibited the largest disparity between ascending and descending stages, with a difference of 700 m (**Table S2**). As illustrated in **Figure S3**, when the HPBL increased from ~900 m to ~1600 m, turbulent mixing transported ground methanol and ethanol upward, leading to a significant increase in alcohol concentrations above 1000 m. In contrast to other OVOCs, acetone and acetaldehyde displayed markedly greater variability above the PBL on Sep. 12th. Both compounds are known to form secondarily through atmospheric oxidation (Holzinger et al., 2005; de Gouw et al., 2004; Wu et al., 2020a), which likely contributes to their less uniform vertical distribution and larger variability at higher altitudes.

For biogenic VOCs, isoprene and monoterpenes are both primarily emitted from biogenic sources, while MVK and MACR are secondary oxidation products of isoprene (Canaval et al., 2020; Cappellin et al., 2019). Across all flight measurements, the vertical distribution patterns of MVK and MACR were quite similar to those observed for alcohols and most aromatic hydrocarbons. In contrast, the vertical profiles of isoprene and monoterpenes varied significantly between flights. Decreasing trends with altitude were found on Sep. 9th (**Figure S2**), Sep. 13th (**Figure S4**), and Sep. 14th (**Figure S5**). On Sep. 12th (**Figure S3**), there were no significant vertical variations of isoprene and monoterpenes across the altitudes. Notably, during the flight on Sep. 15th (**Figure S6**), concentration enhancements can be seen at altitudes above 2000 m, suggesting a potential contribution from atmospheric transport.

The averaged VOC concentrations measured below and above the PBL are compared in the scatter plot shown in **Figure 5**. To account for the variation of HPBL, data points above and below the grey area in **Figure 4** were used to calculate the averages and corresponding standard deviations. The averaged VOC concentrations below the PBL were consistently higher than those above the PBL, reflecting the combined effects of strong surface source emissions and the chemical oxidation process



during vertical transport. Ethanol exhibited the highest concentration within the PBL with an average of 46.7 ppbv and the largest ratio of 16.5 between below- and above-PBL measurements. For the species with secondary formation, the data points of acetaldehyde, acetone, and MEK lay within the 2-5 ratio range. Above the PBL, the averaged concentrations of aromatic hydrocarbons were all smaller than 0.5 ppbv, among which C8 aromatics showed the highest concentration within the PBL, greater than the average above the PBL by a factor of 8.6, followed by toluene and benzene with factors of 6.6 and 5.4, respectively. Notably, the data points of styrene and monoterpenes clustered near the 1:1 ratio line, and occasionally, the concentrations above the PBL could be higher than the ones within the PBL. Both species are primarily emitted at the surface, so this pattern suggests the transport influence. For isoprene, MVK and MACR, C9 aromatics, C10 aromatics, and acetonitrile, the average concentrations below the PBL were approximately twice as high as those measured above the PBL.

3.2 Differences in VOC vertical distribution in Beijing and Baoding

Two out of the six aerial surveys covered both the Beijing and Baoding areas. The aerial survey on Sep. 14th, 2017 maintained a constant altitude of ~3000 m over Baoding, which prevented the collection of a vertical profile for Baoding. The flight conducted on Jul. 14th, 2019 provided comprehensive vertical distribution data for both cities through systematic altitude variations and therefore, was selected for the comparative analysis of urban VOC profiles. As shown in **Figure S7**, the ascending stage over Beijing was quite short (<10 mins), so the vertical profiles measured during the descending stage at noon were selected to better represent the profiles in Beijing. The spiral descending stage in Baoding was used in the comparative analysis as it had well-designed altitude gradients.

The results of the comparison between the vertical VOC distributions of VOCs in Beijing and Baoding are illustrated in **Figure 6**. The VOC profile over Beijing exhibited notable concentration peaks around ~2500 m altitude, a feature previously observed during the flight on Sep. 9th, 2017 (**Figure S2**). This anomaly will be discussed in **Section 3.3** through the ratio analysis. For Baoding, almost all the VOCs showed increasing trends with altitude, except for MVK and MACR, benzene, and toluene, with stable low levels above 1000 m altitude throughout the observation periods. Unfortunately, the aerial survey didn't capture the VOC surface measurements below



500 m in Baoding, which prevented the comparison between the near-ground VOC levels in both cities. Based on the ground monitoring data from local air quality monitoring stations (**Figure S8**), pollution episodes with ozone exceeding the Level-II NAQS in both Beijing and Baoding were captured on Jul. 14th, 2019. Baoding exhibited much higher ozone concentrations compared to Beijing, indicating more severe photochemical pollution. **Figure 7** presents the comparison between the averaged vertical concentrations of VOCs in Beijing and Baoding during the same altitude range (500-3000 m). Ethanol was found with the highest levels of VOCs measured in the air above both cities (**Figure 7a**), 98 ppbv for Beijing and 153 ppbv for Baoding, respectively. According to the scatter plot in **Figure 7b**, all the data points cluster around the 1:2 line. The VOC concentrations in Baoding were higher than those in Beijing by factors ranging from 1.2 to 3.5 with MEK showing the largest difference, demonstrating consistent VOC enhancement patterns. This VOC enhancement implies a greater precursor reservoir over Baoding, which may accelerate secondary pollutant formation through chemical oxidation production and lead to more severe air pollution.

3.3 The contribution of regional emissions to VOC vertical profiles

Among six aerial surveys in 2017 and 2019, two distinct vertical distributions were noticed, characterized by abrupt VOC concentration enhancements above the PBL. For the aerial survey on Sep. 9th, 2017, the vertical profile of styrene exhibited an inverse gradient, with concentrations increasing from 0.2-0.3 ppbv at ground to peak levels of 0.6-1.0 ppbv at ~3500 m altitude, as shown in **Figure 8a**. Above the ~3500 m altitude, styrene concentration rapidly fell back to levels close to the detection limit by 4000 m. Similar increases at 3500 m were also noticed for methanol, acetonitrile, acetaldehyde, benzene, and C9 aromatics. By plotting the ratios of averaged VOC levels at altitudes of 2500-3500 m to the ones near the ground (0-500 m) in **Figure 8b**, only styrene showed a ratio significantly larger than 1. This anomaly indicates that at altitudes of 2500-3500 m, the VOC levels were influenced by air mass rich in styrene transported from further regions.

We further conducted a correlation analysis with styrene and benzene, as they can be co-emitted from common anthropogenic sources. The paired data points of styrene and benzene are shown in **Figure 8d**, together with ratio ranges representing industrial emissions (Jiang et al., 2023; Zhong et al., 2017), vehicular emissions (Wang et al., 2022), and ratios measured in urban Beijing at the IAP tower (He et al., 2025).



296 The data points were color-coded with altitude. An obvious transition between two
297 subsets of data can be seen as the altitude increases. The data points near the ground are
298 all lying between the lines representing the characteristic ratios of diesel vehicles (slope
299 = 0.32) and gasoline vehicles (slope = 0.08) and are consistent with the ratio observed
300 at the Beijing IAP tower. This indicates the dominant contribution from vehicular
301 emissions for the VOCs near the ground. In contrast, the data points observed with
302 altitudes between 2500-3500 m are located in the characteristic ratio ranges related to
303 industrial emissions, which suggests that the VOCs within this altitude range were
304 greatly impacted by industrial emissions.

305 During the aerial survey on Jul. 14th, 2019, the VOC vertical profiles in the
306 Beijing area (**Figure 6**) showed similar trends with elevated VOC concentrations above
307 2500 m for almost all the VOCs. Analyses were conducted for this aerial survey as
308 shown in **Figure 9**. The vertical levels of acetonitrile (**Figure 9a**), a widely applied
309 tracer for biomass burning, were well above the typical backgrounds of 0.1-0.3 ppbv
310 reported in previous studies (Wu et al., 2016; Wang et al., 2007). The ratios of averaged
311 VOC levels at higher altitudes (2500-3000 m) and lower altitudes (<500 m) were
312 plotted in **Figure 9b**. Unlike the ratios illustrated in **Figure 8**, most VOC species in the
313 aerial survey on Jul. 14th had ratios around 1 or even greater than 2 for MEK, C10
314 aromatics, C9 aromatics, and styrene, showing the impact of significant regional
315 transport. Elevated acetonitrile concentrations above the background might suggest
316 biomass burning contribution. However, using acetonitrile as the biomass burning
317 tracer in urban regions can be problematic (Huangfu et al., 2021; Coggon et al., 2016).
318 Other sources (e.g., vehicular emissions) also emit acetonitrile, potentially interfering
319 with the identification of dominant emission sources (Inomata et al., 2013; Valach et al.,
320 2014). Further correlation analysis was conducted between acetonitrile and benzene in
321 **Figure 9d**. Both are typical pollutants emitted from biomass burning and vehicular
322 emissions, therefore, the specific emission ratio of acetonitrile and benzene for both
323 sources can be used as references in the source analysis. We applied the ratio measured
324 in central Beijing to represent the typical ratio of vehicular emissions. Most of the data
325 points lie within the typical biomass burning ratio range and well above the typical ratio
326 of urban vehicular emissions (slope = 0.74). No clear height-dependent classification
327 can be found, which is distinguished from the analysis in **Figure 8d**.

328 The analysis of two distinct vertical distributions reveals that regional transport
329 of emissions, such as industrial and biomass burning, can significantly influence the



VOC vertical profiles, and the associated chemical processes and environmental impact
deserve further investigation.

4 Conclusion

Aircraft-based observations were conducted to investigate the vertical
distribution of VOCs over Beijing and Baoding, two core cities in the NCP region.
According to the vertical profiles of VOC concentrations, near-surface VOC levels
were generally greater than those at higher altitudes, reflecting strong surface source
emissions and chemical removal. In Beijing, ethanol exhibited the highest
concentration within the PBL with an average of 46.7 ppbv and the largest vertical
gradient with a ratio of 16.5 between the below- and above-PBL averages.

The vertical profiles over Beijing and Baoding were compared. Vertical-
averaged VOCs above Baoding were generally greater than those in Beijing by factors
ranging from 1.2 to 3.5. Increasing trends of concentrations with altitude in Baoding
were observed for most VOC species, excluding MVK and MACR, benzene, and
toluene. This implies richer precursors available for the secondary pollutant formation
above Baoding.

Unlike the general vertical distributions, increases of VOC concentrations above
2500 m altitude were captured in Beijing. According to the ratio analysis, VOC levels
near the surface were mainly emitted from vehicular emissions or under the joint impact
of vehicular and biomass burning emissions. In contrast, the regional transport of
industrial and biomass burning emissions drove the distinct enhancement of VOC
concentration above the PBL.

This study presents vertical profiles of key VOC species up to ~4000 m in the
core area of the NCP region, yielding valuable insights into VOC distribution patterns
within the PBL and in the atmosphere above it. The observed concentration
enhancements underscore the substantial impact of regional transport in shaping
vertical distributions of VOCs. As these VOCs actively engage in the complex chemical
processes above the PBL, the secondary pollutant formation at the higher altitudes
necessitates further investigation.



361 **Data availability.**

362 The data in this article are available from the corresponding author upon
363 reasonable request.

364 **Supplement.**

365 The supplement related to this article is available online

366 **Author contributions.**

367 BY and JS designed the research. JS organized the aerial surveys. WZ, FW, PT,
368 WX, YD, and JS contributed to data collection. YH and ZL performed the data analysis,
369 with contributions from BY, SW, and XH. YH, ZL, and BY prepared the article with
370 contributions from SW, XH, and JS. All the authors reviewed the article.

371 **Competing interests.**

372 The authors declare that they have no known competing financial interests that
373 could have appeared to influence the work reported in this paper.

374 **Financial support.**

375 This work was supported by the National Key R&D Program of China (Grant No.
376 2023YFC3710900, 2023YFC3706103, 2024YFC3013001) and the National Natural
377 Science Foundation of China (Grant No. 42230701, 42121004, 42275188).

378

379



380 **Reference**

- 381 Benish, S. E., He, H., Ren, X., Roberts, S. J., Salawitch, R. J., Li, Z., Wang, F., Wang, Y., Zhang, F., Shao,
382 M., Lu, S., and Dickerson, R. R.: Measurement report: Aircraft observations of ozone, nitrogen oxides,
383 and volatile organic compounds over Hebei Province, China, *Atmospheric Chemistry and Physics*, 20,
384 14523-14545, <https://doi.org/10.5194/acp-20-14523-2020>, 2020.
- 385 Canaval, E., Millet, D. B., Zimmer, I., Nosenko, T., Georgii, E., Partoll, E. M., Fischer, L., Alwe, H. D.,
386 Kulmala, M., Karl, T., Schnitzler, J. P., and Hansel, A.: Rapid conversion of isoprene photooxidation
387 products in terrestrial plants, *Commun Earth Environ*, 1, 44, [https://doi.org/10.1038/s43247-020-00041-](https://doi.org/10.1038/s43247-020-00041-2)
388 [2](https://doi.org/10.1038/s43247-020-00041-2), 2020.
- 389 Cappellin, L., Loreto, F., Biasioli, F., Pastore, P., and McKinney, K.: A mechanism for biogenic
390 production and emission of MEK from MVK decoupled from isoprene biosynthesis, *Atmospheric*
391 *Chemistry and Physics*, 19, 3125-3135, <https://doi.org/10.5194/acp-19-3125-2019>, 2019.
- 392 Chang, X., Wang, S., Zhao, B., Xing, J., Liu, X., Wei, L., Song, Y., Wu, W., Cai, S., Zheng, H., Ding, D.,
393 and Zheng, M.: Contributions of inter-city and regional transport to PM_{2.5} concentrations in the Beijing-
394 Tianjin-Hebei region and its implications on regional joint air pollution control, *Science of The Total*
395 *Environment*, 660, 1191-1200, <https://doi.org/10.1016/j.scitotenv.2018.12.474>, 2019.
- 396 Chen, S., Wang, H., Lu, K., Zeng, L., Hu, M., and Zhang, Y.: The trend of surface ozone in Beijing from
397 2013 to 2019: Indications of the persisting strong atmospheric oxidation capacity, *Atmospheric*
398 *Environment*, 242, <https://doi.org/10.1016/j.atmosenv.2020.117801>, 2020.
- 399 Coggon, M. M., Veres, P. R., Yuan, B., Koss, A., Warneke, C., Gilman, J. B., Lerner, B. M., Peischl, J.,
400 Aikin, K. C., Stockwell, C. E., Hatch, L. E., Ryerson, T. B., Roberts, J. M., Yokelson, R. J., and de Gouw,
401 J. A.: Emissions of nitrogen - containing organic compounds from the burning of herbaceous and
402 arboraceous biomass: Fuel composition dependence and the variability of commonly used nitrile tracers,
403 *Geophysical Research Letters*, 43, 9903-9912, <https://doi.org/10.1002/2016gl070562>, 2016.
- 404 de Gouw, J., Warneke, C., Holzinger, R., Klüpfel, T., and Williams, J.: Inter-comparison between airborne
405 measurements of methanol, acetonitrile and acetone using two differently configured PTR-MS
406 instruments, *International Journal of Mass Spectrometry*, 239, 129-137,
407 <https://doi.org/10.1016/j.ijms.2004.07.025>, 2004.



- 408 Dieu Hien, V. T., Lin, C., Thanh, V. C., Kim Oanh, N. T., Thanh, B. X., Weng, C. E., Yuan, C. S., and
409 Rene, E. R.: An overview of the development of vertical sampling technologies for ambient volatile
410 organic compounds (VOCs), *Journal of Environmental Management*, 247, 401-412,
411 <https://doi.org/10.1016/j.jenvman.2019.06.090>, 2019.
- 412 Fisher, J. A., Jacob, D. J., Travis, K. R., Kim, P. S., Marais, E. A., Chan Miller, C., Yu, K., Zhu, L.,
413 Yantosca, R. M., Sulprizio, M. P., Mao, J., Wennberg, P. O., Crounse, J. D., Teng, A. P., Nguyen, T. B.,
414 St. Clair, J. M., Cohen, R. C., Romer, P., Nault, B. A., Wooldridge, P. J., Jimenez, J. L., Campuzano-Jost,
415 P., Day, D. A., Hu, W., Shepson, P. B., Xiong, F., Blake, D. R., Goldstein, A. H., Misztal, P. K., Hanisco,
416 T. F., Wolfe, G. M., Ryerson, T. B., Wisthaler, A., and Mikoviny, T.: Organic nitrate chemistry and its
417 implications for nitrogen budgets in an isoprene- and monoterpene-rich atmosphere: constraints from
418 aircraft (SEAC4RS) and ground-based (SOAS) observations in the Southeast US, *Atmospheric*
419 *Chemistry and Physics*, 16, 5969-5991, <https://doi.org/10.5194/acp-16-5969-2016>, 2016.
- 420 Forster, E., Bonisch, H., Neumaier, M., Obersteiner, F., Zahn, A., Hilboll, A., Kalisz Hedegaard, A. B.,
421 Daskalakis, N., Poulidis, A. P., Vrekoussis, M., Lichtenstern, M., and Braesicke, P.: Chemical and
422 dynamical identification of emission outflows during the HALO campaign EMERGE in Europe and Asia,
423 *Atmospheric Chemistry and Physics*, 23, 1893-1918, <https://doi.org/10.5194/acp-23-1893-2023>, 2023.
- 424 Gao, Y., Wang, H., Yuan, L., Jing, S., Yuan, B., Shen, G., Zhu, L., Koss, A., Li, Y., Wang, Q., Huang, D.
425 D., Zhu, S., Tao, S., Lou, S., and Huang, C.: Measurement report: Underestimated reactive organic gases
426 from residential combustion – insights from a near-complete speciation, *Atmospheric Chemistry and*
427 *Physics*, 23, 6633-6646, <https://doi.org/10.5194/acp-23-6633-2023>, 2023.
- 428 Han, F., Xu, J., He, Y., Dang, H., Yang, X., and Meng, F.: Vertical structure of foggy haze over the
429 Beijing–Tianjin–Hebei area in January 2013, *Atmospheric Environment*, 139, 192-204,
430 <https://doi.org/10.1016/j.atmosenv.2016.05.030>, 2016.
- 431 He, X., Yuan, B., Huangfu, Y., Gouw, J. d., Wang, S., Yang, S., Peng, Y., Parrish, D. D., Li, X., Chang,
432 M., Mo, Z., Min, K.-E., Nam, W., Chen, Y., Zhang, X., Qi, J., Xie, Q., Chen, W., Guenther, A., Wang, X.,
433 Worsnop, D., Karl, T., and Shao, M.: The critical role of urban greening on managing air quality in cities,
434 Under review, 2025.



- 435 Holzinger, R., Williams, J., Salisbury, G., Klüpfel, T., Reus, M. d., Traub, M., Crutzen, P. J., and
436 Lelieveld, J.: Oxygenated compounds in aged biomass burning plumes over the Eastern Mediterranean:
437 evidence for strong secondary production of methanol and acetone, *Atmospheric Chemistry and Physics*,
438 5, <https://doi.org/10.5194/acp-5-39-2005>, 2005.
- 439 Huangfu, Y., Yuan, B., Wang, S., Wu, C., He, X., Qi, J., de Gouw, J., Warneke, C., Gilman, J. B., Wisthaler,
440 A., Karl, T., Graus, M., Jobson, B. T., and Shao, M.: Revisiting Acetonitrile as Tracer of Biomass Burning
441 in Anthropogenic - Influenced Environments, *Geophysical Research Letters*, 48,
442 <https://doi.org/10.1029/2020gl092322>, 2021.
- 443 Inomata, S., Tanimoto, H., Fujitani, Y., Sekimoto, K., Sato, K., Fushimi, A., Yamada, H., Hori, S.,
444 Kumazawa, Y., Shimono, A., and Hikida, T.: On-line measurements of gaseous nitro-organic compounds
445 in diesel vehicle exhaust by proton-transfer-reaction mass spectrometry, *Atmospheric Environment*, 73,
446 195-203, <https://doi.org/10.1016/j.atmosenv.2013.03.035>, 2013.
- 447 Jiang, C., Pei, C., Cheng, C., Shen, H., Zhang, Q., Lian, X., Xiong, X., Gao, W., Liu, M., Wang, Z.,
448 Huang, B., Tang, M., Yang, F., Zhou, Z., and Li, M.: Emission factors and source profiles of volatile
449 organic compounds from typical industrial sources in Guangzhou, China, *Science of the Total*
450 *Environment*, 869, 161758, <https://doi.org/10.1016/j.scitotenv.2023.161758>, 2023.
- 451 Karion, A., Sweeney, C., Kort, E. A., Shepson, P. B., Brewer, A., Cambaliza, M., Conley, S. A., Davis,
452 K., Deng, A., Hardesty, M., Herndon, S. C., Lauvaux, T., Lavoie, T., Lyon, D., Newberger, T., Petron, G.,
453 Rella, C., Smith, M., Wolter, S., Yacovitch, T. I., and Tans, P.: Aircraft-Based Estimate of Total Methane
454 Emissions from the Barnett Shale Region, *Environmental Science & Technology*, 49, 8124-8131,
455 <https://doi.org/10.1021/acs.est.5b00217>, 2015.
- 456 Kwak, K.-H., Lee, S.-H., Kim, A. Y., Park, K.-C., Lee, S.-E., Han, B.-S., Lee, J., and Park, Y.-S.: Daytime
457 Evolution of Lower Atmospheric Boundary Layer Structure: Comparative Observations between a 307-
458 m Meteorological Tower and a Rotary-Wing UAV, *Atmosphere*, 11,
459 <https://doi.org/10.3390/atmos1111142>, 2020.
- 460 Le, T., Wang, Y., Liu, L., Yang, J., Yung, Y. L., Li, G., and Seinfeld, J. H.: Unexpected air pollution with
461 marked emission reductions during the COVID-19 outbreak in China, *Science*, 369, 702-706,
462 <https://doi.org/10.1126/science.abb7431>, 2020.



463 Li, K., Jacob, D. J., Liao, H., Shen, L., Zhang, Q., and Bates, K. H.: Anthropogenic drivers of 2013–2017
464 trends in summer surface ozone in China, Proceedings of the National Academy of Sciences of the United
465 States of America, 116, 422–427, <https://doi.org/10.1073/pnas.1812168116>, 2019a.

466 Li, M., Zhang, Q., Zheng, B., Tong, D., Lei, Y., Liu, F., Hong, C., Kang, S., Yan, L., Zhang, Y., Bo, Y.,
467 Su, H., Cheng, Y., and He, K.: Persistent growth of anthropogenic non-methane volatile organic
468 compound (NMVOC) emissions in China during 1990–2017: drivers, speciation and ozone formation
469 potential, Atmospheric Chemistry and Physics, 19, 8897–8913, [https://doi.org/10.5194/acp-19-8897-](https://doi.org/10.5194/acp-19-8897-2019)
470 [2019](https://doi.org/10.5194/acp-19-8897-2019), 2019b.

471 Li, X.-B., Yuan, B., Huangfu, Y., Yang, S., Song, X., Qi, J., He, X., Wang, S., Chen, Y., Yang, Q., Song,
472 Y., Peng, Y., Tang, G., Gao, J., and Shao, M.: Vertical changes in volatile organic compounds (VOCs)
473 and impacts on photochemical ozone formation, Atmospheric Chemistry and Physics, 25, 2459–2472,
474 <https://doi.org/10.5194/acp-25-2459-2025>, 2024.

475 Li, X. B., Yuan, B., Wang, S., Wang, C., Lan, J., Liu, Z., Song, Y., He, X., Huangfu, Y., Pei, C., Cheng,
476 P., Yang, S., Qi, J., Wu, C., Huang, S., You, Y., Chang, M., Zheng, H., Yang, W., Wang, X., and Shao, M.:
477 Variations and sources of volatile organic compounds (VOCs) in urban region: insights from
478 measurements on a tall tower, Atmospheric Chemistry and Physics, 22, 10567–10587,
479 <https://doi.org/10.5194/acp-22-10567-2022>, 2022a.

480 Li, Z., Yu, S., Li, M., Chen, X., Zhang, Y., Song, Z., Li, J., Jiang, Y., Liu, W., Li, P., and Zhang, X.: The
481 Modeling Study about Impacts of Emission Control Policies for Chinese 14th Five-Year Plan on PM_{2.5}
482 and O₃ in Yangtze River Delta, China, Atmosphere, 13, 26, <https://doi.org/10.3390/atmos13010026>,
483 2022b.

484 Liu, K., Quan, J., Mu, Y., Zhang, Q., Liu, J., Gao, Y., Chen, P., Zhao, D., and Tian, H.: Aircraft
485 measurements of BTEX compounds around Beijing city, Atmospheric Environment, 73, 11–15,
486 <https://doi.org/10.1016/j.atmosenv.2013.02.050>, 2013.

487 Liu, Q., Ding, D., Huang, M., Tian, P., Zhao, D., Wang, F., Li, X., Bi, K., Sheng, J., Zhou, W., Liu, D.,
488 Huang, R., and Zhao, C.: A study of elevated pollution layer over the North China Plain using aircraft
489 measurements, Atmospheric Environment, 190, 188–194,
490 <https://doi.org/10.1016/j.atmosenv.2018.07.024>, 2018.



- 491 Liu, Y., Wang, H., Jing, S., Gao, Y., Peng, Y., Lou, S., Cheng, T., Tao, S., Li, L., Li, Y., Huang, D., Wang,
492 Q., and An, J.: Characteristics and sources of volatile organic compounds (VOCs) in Shanghai during
493 summer: Implications of regional transport, *Atmospheric Environment*, 215,
494 <https://doi.org/10.1016/j.atmosenv.2019.116902>, 2019.
- 495 Lu, X., Zhang, L., Chen, Y., Zhou, M., Zheng, B., Li, K., Liu, Y., Lin, J., Fu, T.-M., and Zhang, Q.:
496 Exploring 2016–2017 surface ozone pollution over China: source contributions and meteorological
497 influences, *Atmospheric Chemistry and Physics*, 19, 8339–8361, [https://doi.org/10.5194/acp-19-8339-](https://doi.org/10.5194/acp-19-8339-2019)
498 [2019](https://doi.org/10.5194/acp-19-8339-2019), 2019.
- 499 Lu, X., Zhang, L., Wang, X., Gao, M., Li, K., Zhang, Y., Yue, X., and Zhang, Y.: Rapid Increases in
500 Warm-Season Surface Ozone and Resulting Health Impact in China Since 2013, *Environmental Science*
501 *& Technology Letters*, 7, 240–247, <https://doi.org/10.1021/acs.estlett.0c00171>, 2020.
- 502 Mao, Z., Bai, Y., and Meng, F.: How can China achieve the energy and environmental targets in the 14th
503 and 15th five-year periods? A perspective of economic restructuring, *Sustainable Production and*
504 *Consumption*, 27, 2022–2036, <https://doi.org/10.1016/j.spc.2021.05.005>, 2021.
- 505 Peng, Z.-R., Wang, D., Wang, Z., Gao, Y., and Lu, S.: A study of vertical distribution patterns of PM_{2.5}
506 concentrations based on ambient monitoring with unmanned aerial vehicles: A case in Hangzhou, China,
507 *Atmospheric Environment*, 123, 357–369, <https://doi.org/10.1016/j.atmosenv.2015.10.074>, 2015.
- 508 Ren, X., Salmon, O. E., Hansford, J. R., Ahn, D., Hall, D., Benish, S. E., Stratton, P. R., He, H., Sahu, S.,
509 Grimes, C., Heimbürger, A. M. F., Martin, C. R., Cohen, M. D., Stunder, B., Salawitch, R. J., Ehrman, S.
510 H., Shepson, P. B., and Dickerson, R. R.: Methane Emissions From the Baltimore–Washington Area
511 Based on Airborne Observations: Comparison to Emissions Inventories, *Journal of Geophysical*
512 *Research: Atmospheres*, 123, 8869–8882, <https://doi.org/10.1029/2018jd028851>, 2018.
- 513 Sangiorgi, G., Ferrero, L., Perrone, M. G., Bolzacchini, E., Duane, M., and Larsen, B. R.: Vertical
514 distribution of hydrocarbons in the low troposphere below and above the mixing height: Tethered balloon
515 measurements in Milan, Italy, *Environmental Pollution*, 159, 3545–3552,
516 <https://doi.org/10.1016/j.envpol.2011.08.012>, 2011.



- 517 Shi, H., Critto, A., Torresan, S., and Gao, Q.: The Temporal and Spatial Distribution Characteristics of
518 Air Pollution Index and Meteorological Elements in Beijing, Tianjin, and Shijiazhuang, China, Integrated
519 Environmental Assessment and Management, 14, 710-721, <https://doi.org/10.1002/ieam.4067>, 2018.
- 520 Squires, F. A., Nemitz, E., Langford, B., Wild, O., Drysdale, W. S., Acton, W. J. F., Fu, P., Grimmond, C.
521 S. B., Hamilton, J. F., Hewitt, C. N., Hollaway, M., Kotthaus, S., Lee, J., Metzger, S., Pisingtha-Durden,
522 N., Shaw, M., Vaughan, A. R., Wang, X., Wu, R., Zhang, Q., and Zhang, Y.: Measurements of traffic-
523 dominated pollutant emissions in a Chinese megacity, Atmospheric Chemistry and Physics, 20, 8737-
524 8761, <https://doi.org/10.5194/acp-20-8737-2020>, 2020.
- 525 Sun, J., Wang, Y., Wu, F., Tang, G., Wang, L., Wang, Y., and Yang, Y.: Vertical characteristics of VOCs
526 in the lower troposphere over the North China Plain during pollution periods, Environmental Pollution,
527 236, 907-915, <https://doi.org/10.1016/j.envpol.2017.10.051>, 2018.
- 528 Valach, A. C., Langford, B., Nemitz, E., MacKenzie, A. R., and Hewitt, C. N.: Concentrations of selected
529 volatile organic compounds at kerbside and background sites in central London, Atmospheric
530 Environment, 95, 456-467, <https://doi.org/10.1016/j.atmosenv.2014.06.052>, 2014.
- 531 Vo, T. D., Lin, C., Weng, C. E., Yuan, C. S., Lee, C. W., Hung, C. H., Bui, X. T., Lo, K. C., and Lin, J.
532 X.: Vertical stratification of volatile organic compounds and their photochemical product formation
533 potential in an industrial urban area, Journal of Environmental Management, 217, 327-336,
534 <https://doi.org/10.1016/j.jenvman.2018.03.101>, 2018.
- 535 Vogelesang, D. H. P., and Holtslag, A. A. M.: Evaluation and model impacts of alternative boundary-
536 layer height formulations, Boundary-Layer Meteorology, 81, 245-269,
537 <https://doi.org/10.1007/BF02430331>, 1996.
- 538 Wang, M., Shao, M., Chen, W., Yuan, B., Lu, S., Zhang, Q., Zeng, L., and Wang, Q.: A temporally and
539 spatially resolved validation of emission inventories by measurements of ambient volatile organic
540 compounds in Beijing, China, Atmospheric Chemistry and Physics, 14, 5871-5891,
541 <https://doi.org/10.5194/acp-14-5871-2014>, 2014.
- 542 Wang, Q., Shao, M., Liu, Y., William, K., Paul, G., Li, X., Liu, Y., and Lu, S.: Impact of biomass burning
543 on urban air quality estimated by organic tracers: Guangzhou and Beijing as cases, Atmospheric
544 Environment, 41, 8380-8390, <https://doi.org/10.1016/j.atmosenv.2007.06.048>, 2007.



- 545 Wang, S., Yuan, B., Wu, C., Wang, C., Li, T., He, X., Huangfu, Y., Qi, J., Li, X.-B., Sha, Q. e., Zhu, M.,
546 Lou, S., Wang, H., Karl, T., Graus, M., Yuan, Z., and Shao, M.: Oxygenated volatile organic compounds
547 (VOCs) as significant but varied contributors to VOC emissions from vehicles, *Atmospheric Chemistry*
548 *and Physics*, 22, 9703-9720, <https://doi.org/10.5194/acp-22-9703-2022>, 2022.
- 549 Wang, S., Yuan, B., He, X., Cui, R., Song, X., Chen, Y., Wu, C., Wang, C., Huangfu, Y., Li, X.-B., Wang,
550 B., and Shao, M.: Emission characteristics of reactive organic gases (ROGs) from industrial volatile
551 chemical products (VCPs) in the Pearl River Delta (PRD), China, *Atmospheric Chemistry and Physics*,
552 24, 7101-7121, <https://doi.org/10.5194/acp-24-7101-2024>, 2024.
- 553 Wang, Z., Zhang, P., Pan, L., Qian, Y., Li, Z., Li, X., Guo, C., Zhu, X., Xie, Y., and Wei, Y.: Ambient
554 Volatile Organic Compound Characterization, Source Apportionment, and Risk Assessment in Three
555 Megacities of China in 2019, *Toxics*, 11, <https://doi.org/10.3390/toxics11080651>, 2023.
- 556 Wilde, S. E., Dominutti, P. A., Allen, G., Andrews, S. J., Bateson, P., Bauguittie, S. J. B., Burton, R. R.,
557 Colfescu, I., France, J., Hopkins, J. R., Huang, L., Jones, A. E., Lachlan-Cope, T., Lee, J. D., Lewis, A.
558 C., Mobbs, S. D., Weiss, A., Young, S., and Purvis, R. M.: Speciation of VOC emissions related to
559 offshore North Sea oil and gas production, *Atmospheric Chemistry and Physics*, 21, 3741-3762,
560 <https://doi.org/10.5194/acp-21-3741-2021>, 2021.
- 561 Wu, C., Wang, C., Wang, S., Wang, W., Yuan, B., Qi, J., Wang, B., Wang, H., Wang, C., Song, W., Wang,
562 X., Hu, W., Lou, S., Ye, C., Peng, Y., Wang, Z., Huangfu, Y., Xie, Y., Zhu, M., Zheng, J., Wang, X., Jiang,
563 B., Zhang, Z., and Shao, M.: Measurement report: Important contributions of oxygenated compounds to
564 emissions and chemistry of volatile organic compounds in urban air, *Atmospheric Chemistry and Physics*,
565 20, 14769-14785, <https://doi.org/10.5194/acp-20-14769-2020>, 2020a.
- 566 Wu, J., Gao, S., Chen, X., Yang, Y., Fu, Q.-Y., Che, X., and Jiao, Z.: Source Profiles and Impact of Volatile
567 Organic Compounds in the Coating Manufacturing Industry, *Environmental Science*, 41, 1582-1588,
568 <https://doi.org/10.13227/j.hjlx.201908203>, 2020b.
- 569 Wu, R., Li, J., Hao, Y., Li, Y., Zeng, L., and Xie, S.: Evolution process and sources of ambient volatile
570 organic compounds during a severe haze event in Beijing, China, *Science of The Total Environment*,
571 560-561, 62-72, <https://doi.org/10.1016/j.scitotenv.2016.04.030>, 2016.



- 572 Xue, L., Wang, T., Simpson, I. J., Ding, A., Gao, J., Blake, D. R., Wang, X., Wang, W., Lei, H., and Jin,
573 D.: Vertical distributions of non-methane hydrocarbons and halocarbons in the lower troposphere over
574 northeast China, *Atmospheric Environment*, 45, <https://doi.org/10.1016/j.atmosenv.2011.08.072>, 2011.
- 575 Yang, Q., Li, X.-B., Yuan, B., Zhang, X., Huangfu, Y., Yang, L., He, X., Qi, J., and Shao, M.:
576 Measurement report: Enhanced photochemical formation of formic and isocyanic acids in urban regions
577 aloft – insights from tower-based online gradient measurements, *Atmospheric Chemistry and Physics*,
578 24, 6865-6882, <https://doi.org/10.5194/acp-24-6865-2024>, 2024.
- 579 Yao, D., Tang, G., Wang, Y., Yang, Y., Wang, Y., Liu, Y., Yu, M., Liu, Y., Yu, H., Liu, J., Hu, B., Wang,
580 P., and Wang, Y.: Oscillation cumulative volatile organic compounds on the northern edge of the North
581 China Plain: Impact of mountain-plain breeze, *Science of The Total Environment*, 821, 153541,
582 <https://doi.org/10.1016/j.scitotenv.2022.153541>, 2022.
- 583 Yuan, B., Shao, M., de Gouw, J., Parrish, D. D., Lu, S., Wang, M., Zeng, L., Zhang, Q., Song, Y., Zhang,
584 J., and Hu, M.: Volatile organic compounds (VOCs) in urban air: How chemistry affects the interpretation
585 of positive matrix factorization (PMF) analysis, *Journal of Geophysical Research: Atmospheres*, 117,
586 n/a-n/a, <https://doi.org/10.1029/2012jd018236>, 2012.
- 587 Yuan, B., Koss, A. R., Warneke, C., Coggon, M., Sekimoto, K., and de Gouw, J. A.: Proton-Transfer-
588 Reaction Mass Spectrometry: Applications in Atmospheric Sciences, *Chemical Reviews*, 117, 13187-
589 13229, <https://doi.org/10.1021/acs.chemrev.7b00325>, 2017.
- 590 Zhang, H., Zhang, Y., Huang, Z., Acton, W. J. F., Wang, Z., Nemitz, E., Langford, B., Mullinger, N.,
591 Davison, B., Shi, Z., Liu, D., Song, W., Yang, W., Zeng, J., Wu, Z., Fu, P., Zhang, Q., and Wang, X.:
592 Vertical profiles of biogenic volatile organic compounds as observed online at a tower in Beijing, *Journal*
593 *of Environmental Sciences*, 95, 33-42, <https://doi.org/10.1016/j.jes.2020.03.032>, 2020.
- 594 Zhang, K., Xiu, G., Zhou, L., Bian, Q., Duan, Y., Fei, D., Wang, D., and Fu, Q.: Vertical distribution of
595 volatile organic compounds within the lower troposphere in late spring of Shanghai, *Atmospheric*
596 *Environment*, 186, 150-157, <https://doi.org/10.1016/j.atmosenv.2018.03.044>, 2018.
- 597 Zhang, K., Zhou, L., Fu, Q., Yan, L., Bian, Q., Wang, D., and Xiu, G.: Vertical distribution of ozone over
598 Shanghai during late spring: A balloon-borne observation, *Atmospheric Environment*, 208, 48-60,
599 <https://doi.org/10.1016/j.atmosenv.2019.03.011>, 2019.



600 Zhang, Y., Gao, Z., Li, D., Li, Y., Zhang, N., Zhao, X., and Chen, J.: On the computation of planetary
601 boundary-layer height using the bulk Richardson number method, *Geoscientific Model Development*, 7,
602 2599-2611, <https://doi.org/10.5194/gmd-7-2599-2014>, 2014.

603 Zhao, D., Huang, M., Tian, P., He, H., Lowe, D., Zhou, W., Sheng, J., Wang, F., Bi, K., Kong, S., Yang,
604 Y., Liu, Q., Liu, D., and Ding, D.: Vertical characteristics of black carbon physical properties over Beijing
605 region in warm and cold seasons, *Atmospheric Environment*, 213, 296-310,
606 <https://doi.org/10.1016/j.atmosenv.2019.06.007>, 2019.

607 Zhao, D., Liu, D., Yu, C., Tian, P., Hu, D., Zhou, W., Ding, S., Hu, K., Sun, Z., Huang, M., Huang, Y.,
608 Yang, Y., Wang, F., Sheng, J., Liu, Q., Kong, S., Li, X., He, H., and Ding, D.: Vertical evolution of black
609 carbon characteristics and heating rate during a haze event in Beijing winter, *Science of The Total*
610 *Environment*, 709, <https://doi.org/10.1016/j.scitotenv.2019.136251>, 2020.

611 Zhao, R., Yin, B., Zhang, N., Wang, J., Geng, C., Wang, X., Han, B., Li, K., Li, P., Yu, H., Yang, W., and
612 Bai, Z.: Aircraft-based observation of gaseous pollutants in the lower troposphere over the Beijing-
613 Tianjin-Hebei region, *Science of The Total Environment*, 773,
614 <https://doi.org/10.1016/j.scitotenv.2020.144818>, 2021.

615 Zhong, Z., Sha, Q., Zheng, J., Yuan, Z., Gao, Z., Ou, J., Zheng, Z., Li, C., and Huang, Z.: Sector-based
616 VOCs emission factors and source profiles for the surface coating industry in the Pearl River Delta region
617 of China, *Science of the Total Environment*, 583, 19-28, <https://doi.org/10.1016/j.scitotenv.2016.12.172>,
618 2017.

619

620 **Table 1.** Detailed information for different flight routes during different aerial surveys in Sep. 2017 and Jul. 2019.

Route num	Main a	Main altitude (Date	Profile time*	
				Ascending	Descending st
Route 1	Beijin	~3800	Sep. 09, 201	12:06-12:	12:31-16:4
Route 2	Beijin	~3800	Sep. 12, 201	12:16-12:	12:55-16:4
Route 3	Beijin	~3800	Sep. 13, 201	13:35-14:	14:30-16:4
Route 4	Beijin	~3700	Sep. 15, 201	10:36-11:	11:00-13:4
Route 5	Beijin	~2500/~2800	Sep. 14, 201	12:31-12:	16:00-16:4
	Baodin	2200-3500	Sep. 14, 201	-	-
Route 6	Beijin	~3100	Jul. 14, 2019	9:41-10:	11:43-12:
	Baodin	~3090	Jul. 14, 2019	11:21-11:	10:18-11:

621 Note: * Profile time is the local time.

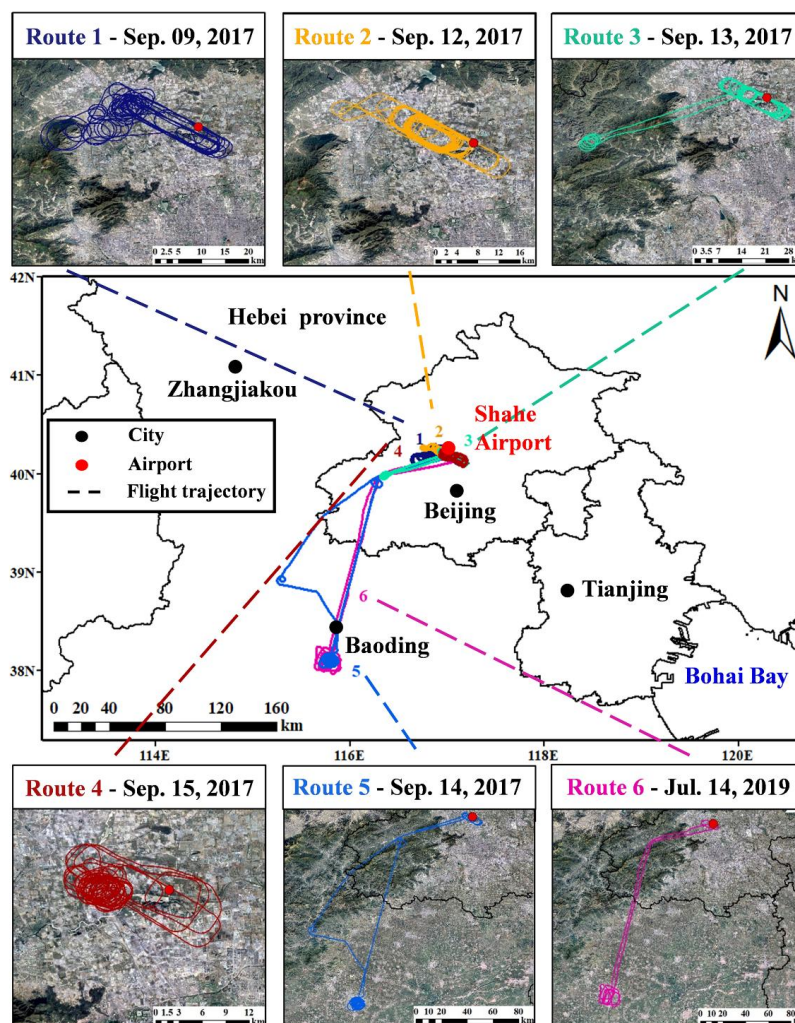


Figure 1. Flight trajectories during different aerial surveys in Sep. 2017 and Jul. 2019. Figures were made by Meteolnfo software. The satellite images were downloaded from © Google Earth and edited in ArcGIS 10.8.

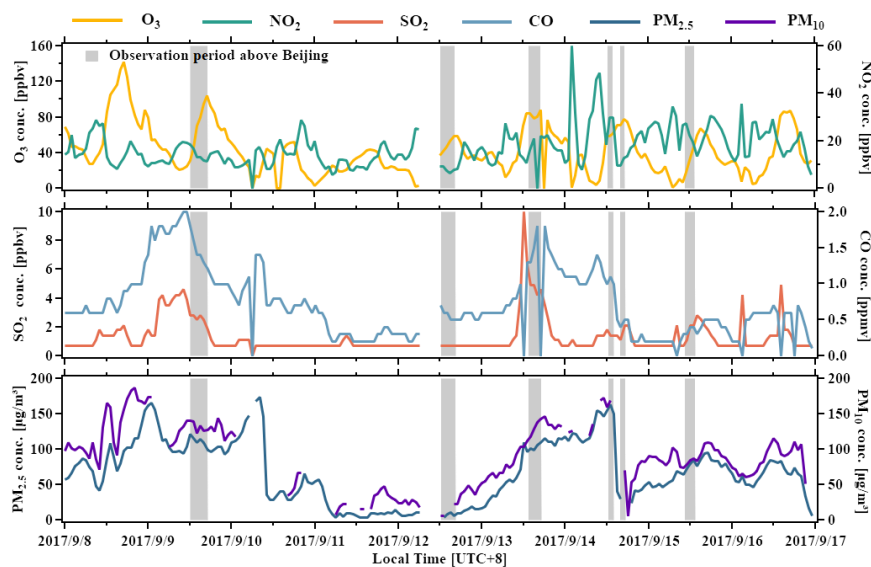
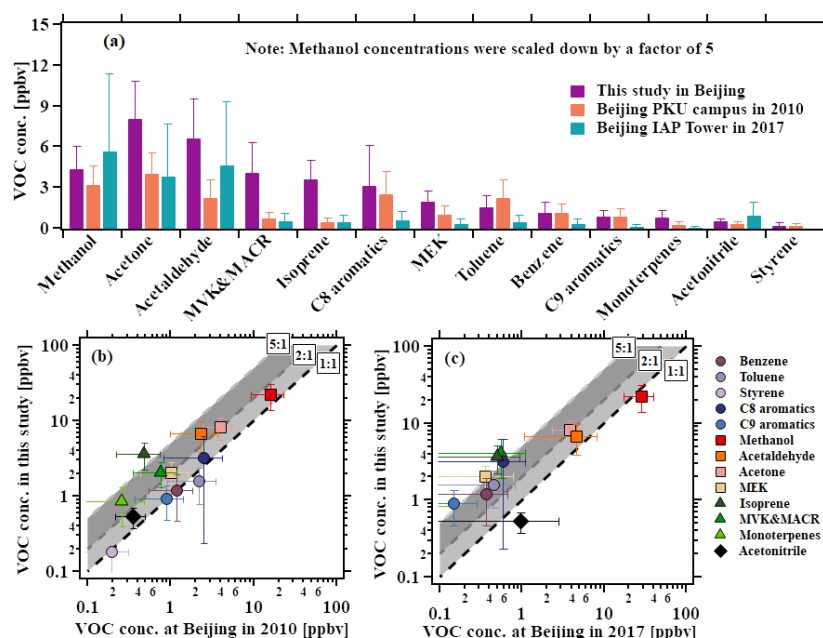


Figure 2. Time series of criteria pollutants including ozone, NO₂, SO₂, CO, PM_{2.5}, and PM₁₀ from Sep. 8th to 16th, 2017. Data is obtained from Changping Town stations, the closest national air quality monitoring stations to the airport. Shaded areas indicate the observation periods.



635

636 **Figure 3.** Comparison of averaged VOC concentrations below the PBL in this study
637 and those measured in Beijing in 2010 (Yuan et al., 2012) and 2017 (Squires et al.,
638 2020). Methanol concentrations were scaled down by a factor of 5 to improve
639 visualization in (a). Scatter plots were also shown in (b) and (c). Error bars indicate the
640 standard deviations. Reference lines are shown with shading to illustrate the differences.

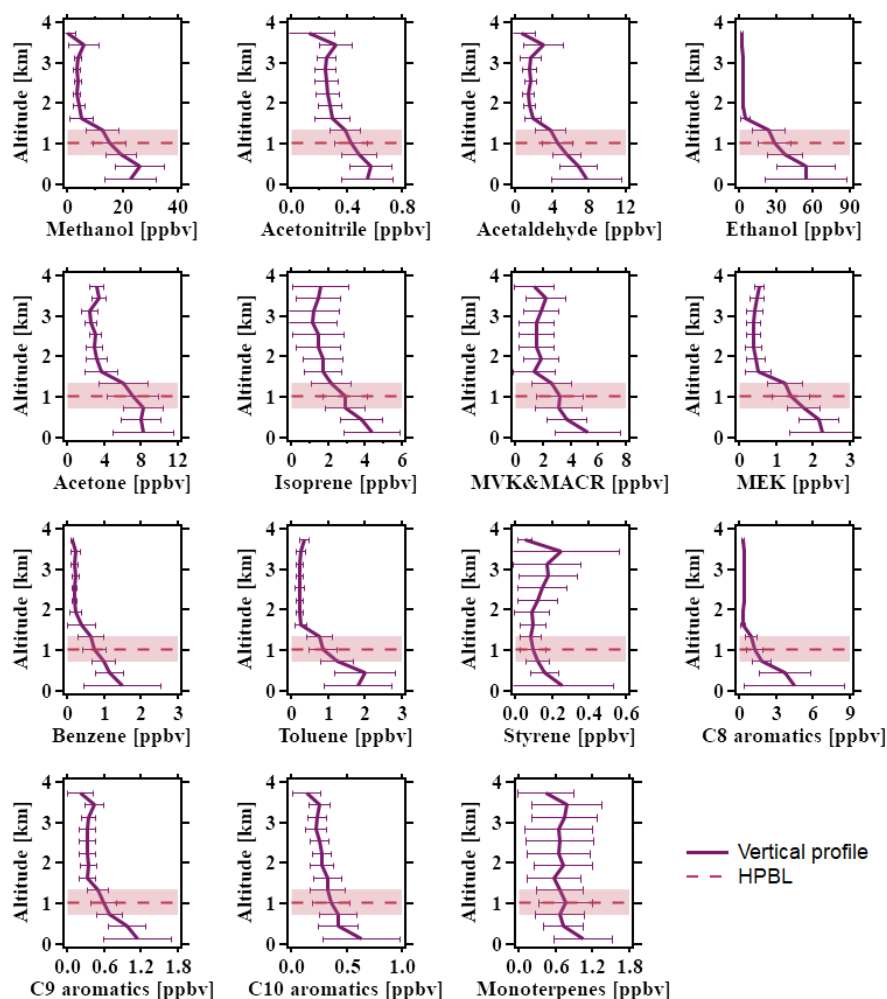
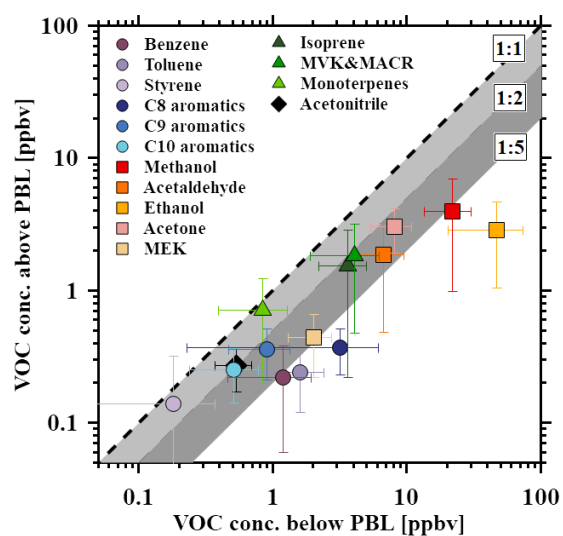
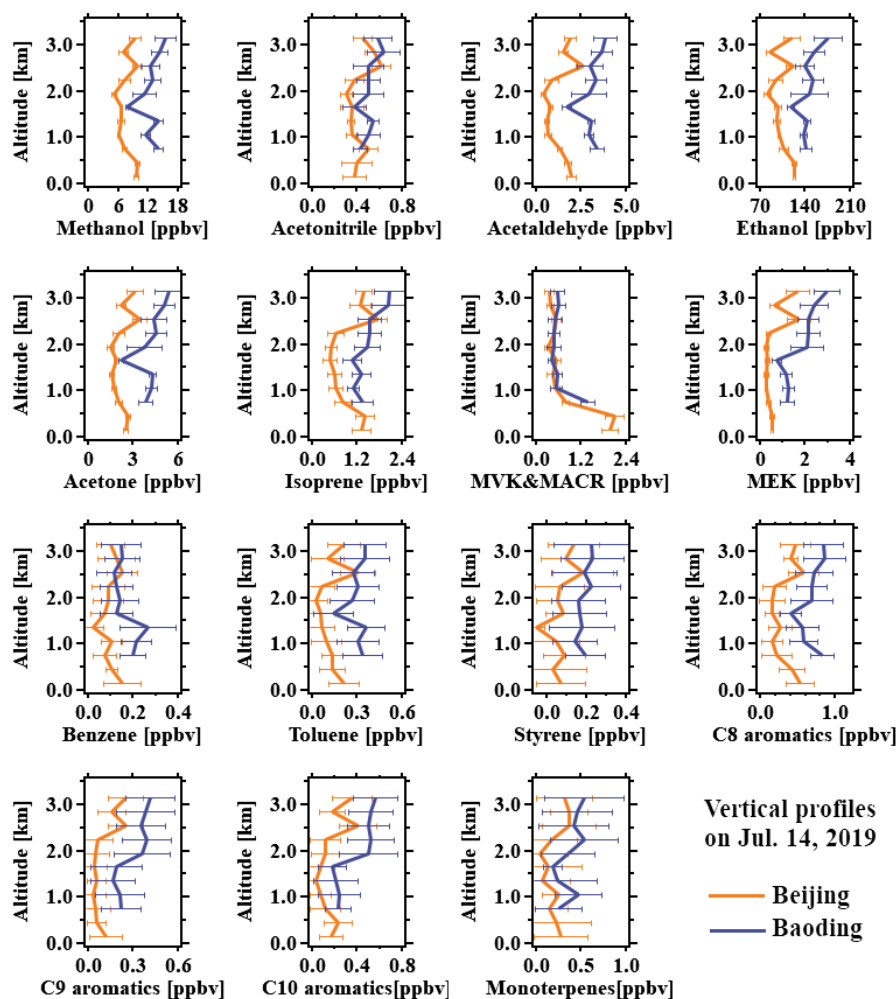


Figure 4. Averaged vertical profile (purple line) of VOCs in five aerial surveys above the Beijing area in Sep. 2017 with error bar. The red dashed line is the average of the HPBL, with the light red area showing the variation range of one standard deviation.



646
647 **Figure 5.** Scatter plot of the averaged VOC concentrations in Beijing below and above
648 the PBL in Sep. 2017. Error bars indicate the standard deviations. Reference lines are
649 shown with shading to illustrate the differences.
650



651

652 **Figure 6.** Comparison of vertical profiles of VOCs in Beijing (in orange) and Baoding
 653 (in blue) during the aerial survey on Jul. 14th, 2019, with error bars. The data measured
 654 during the descending stages above both cities were plotted.

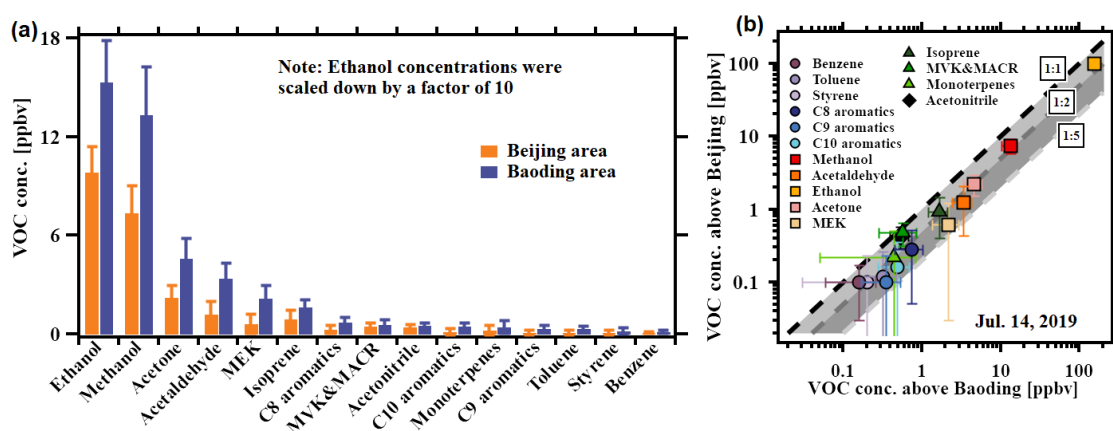
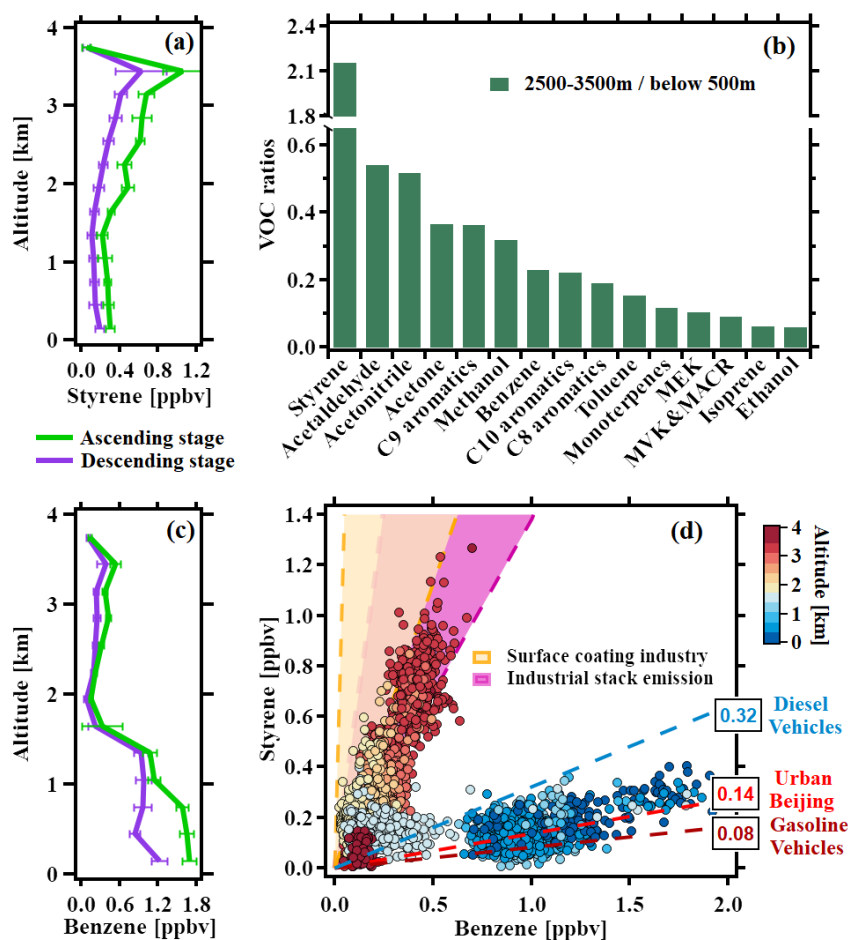
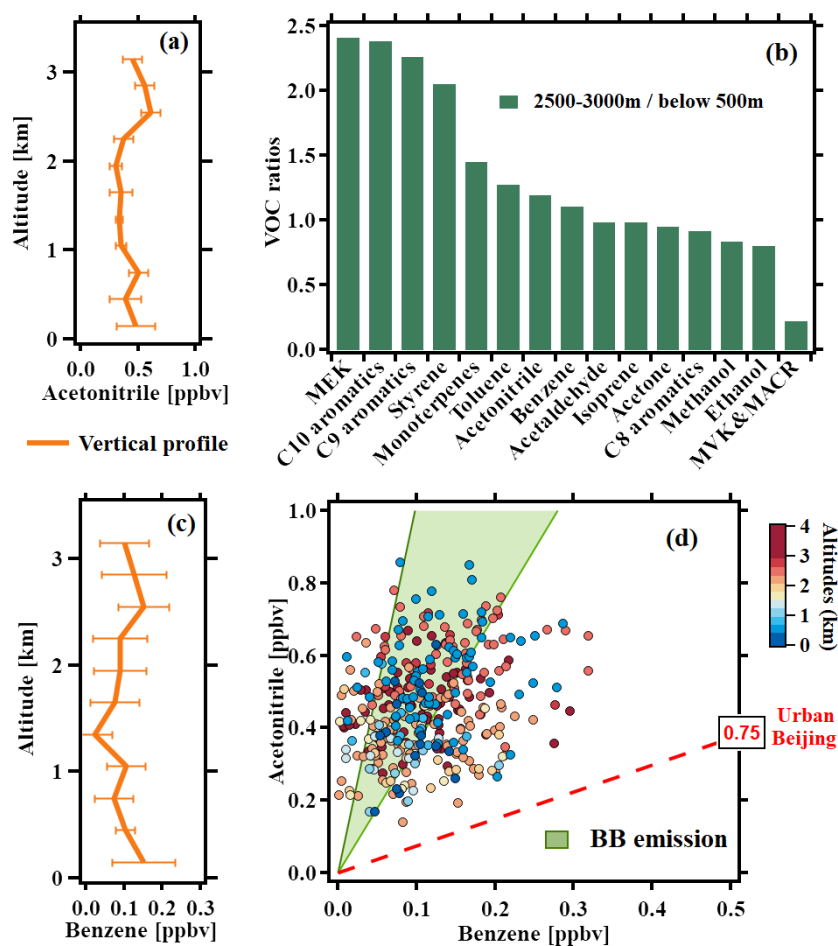


Figure 7. Comparison of averaged VOC vertical concentrations in Beijing and Baoding during the aerial survey on Jul. 14th, 2019. The data measured within the same altitude range (500 m - 3000 m) were averaged. Ethanol concentrations were scaled down by a factor of 10 to improve visualization in (a). The scatter plot was made in (b). Error bars indicate the standard deviations. Reference lines are shown with shading to illustrate the differences.



661
662 **Figure 8.** Analysis of the vertical profiles of styrene (a) and benzene (c) during
663 ascending (in green) and descending (in purple) stages with error bars on Sep. 9th, 2017.
664 (b) The ratios of each VOC species measured between 2500-3500 m and below 500 m.
665 (d) The correlation analysis between styrene and benzene using the profiles. All the
666 data points were color-coded with altitudes. The area with orange shadows represents
667 the ratio ranges of styrene and benzene in the surface coating industry (Zhong et al.,
668 2017). The area with purple shadows represents the ratio ranges in typical industrial
669 stack emissions (Jiang et al., 2023). The blue and dark red dashed lines represent ratios
670 of styrene and benzene for diesel and gasoline vehicular emissions, respectively (Wang
671 et al., 2024). The red dashed line represents the ratio measured in urban Beijing at the
672 IAP tower in 2021 (He et al., 2025).



673

674 **Figure 9.** Analysis of the vertical profiles of acetonitrile (a) and benzene (c) with error
675 bars on Jul. 14th, 2019. (b) The ratios of each VOC species measured between 2500-
676 3000 m and below 500 m. (d) The correlation analysis between acetonitrile and benzene
677 using the profiles. All the data points were color-coded with altitudes. The red dashed
678 lines represent ratios in urban Beijing at the IAP tower in 2021 (He et al., 2025). The
679 area with green shadow represents the ratio ranges of acetonitrile and benzene measured
680 in the biomass burning (BB) emissions, including wood, corncob, corn straw, and bean
681 straw (Gao et al., 2023).